frontiers | Frontiers in Earth Science

ORIGINAL RESEARCH
published: 14 June 2022
doi: 10.3389/feart.2022.881762

The Effect of Thermochemical Sulphate Reduction on the Carbon Isotope Ratio of Individual Light Hydrocarbons Associated With Natural Gas

Guoyi Hu[1], Jinhao Guo[1], Lianjie Tian[1], Xiaoqi Wu[2], Jin Su[1], Zhisheng Li[1] and Chenchen Fang[1]*

[1]*Research Institute of Petroleum Exploration and Development, PetroChina, Beijing, China,* [2]*Wuxi Research Institute of Petroleum Geology, Petroleum Exploration and Production Research Institute, Sinopec, Wuxi, China*

To understand the effect of thermochemical sulphate reduction (TSR) on the stable carbon isotopes of light hydrocarbons (LHs) associated with natural gas, 15 gases with varying H_2S content from Ordovician reservoir of the Tazhong gas field (TZ-I) in Tarim Basin and Triassic Leikoupo reservoir of the Zhongba gas field (ZB) in Sichuan Basin were collected. Based on the data from molecular components and stable carbon isotope ratios of the C_1-C_4 alongside the individual LHs (C_6-C_7) in these gases, the origin of natural gas and the effect of TSR on the stable carbon isotope ratio of individual LHs were studied. The $\delta^{13}C$ in ethane (<−28‰), LHs (<−26‰) and the composition distribution characteristic of C_6-C_7 indicated that the gases were oil-associated gases. Moreover, the gas sourness index, defined as $H_2S/(H_2S+\sum C_n)$ demonstrated that the gases from the TZ-I and ZB gas fields were in the early liquid-hydrocarbon-involved and heavy-hydrocarbon-gas-dominated TSR stages, respectively. The comparison of stable carbon isotope ratios of the LHs between the two gas fields revealed that TSR exhibited a complex effect on the carbon isotope values of LHs, but only little effect on 2-methylpentane (2-MP) and 3-methylpentane (3-MP). The $\delta^{13}C$ values of benzene (BEN) and toluene (TOL) were -28.3‰ and -29.4‰ in the TZ-I and -27.7‰ and -28.1‰ in the ZB gas field. The stable carbon isotope ratios of BEN and TOL in ZB gas field exhibited more enriched ^{13}C than those in TZ-I gas field, likely driven by TSR. Meanwhile, cycloalkanes, such as methyl cyclopentane (MCP), cyclohexane (CH), and methylcyclohexane (MCH), enriched ^{13}C with TSR process and displayed a greater trend than aromatic compounds, about 2‰. Therefore, the influence of TSR on the carbon isotopes of individual LHs should be considered while using the stable carbon isotope ratio of cycloalkanes, BEN, and TOL to identify the genetic type and source of marine natural gas, especially at the cross plot ($\delta^{13}C$ = −24‰) of coal-derived gas and oil-associated gas.

Keywords: light hydrocarbons, carbon isotope, thermochemical sulfate reduction, natural gas, Zhongba gas field, Tazhong|gas field

OPEN ACCESS

Edited by:
Tongwei Zhang,
University of Texas at Austin,
United States

Reviewed by:
Weichao Wu,
Stockholm University, Sweden
Amzad Hussain Laskar,
Physical Research Laboratory, India

****Correspondence:***
Guoyi Hu
huguoyi69@petrochina.com.cn

Specialty section:
This article was submitted to Geochemistry, a section of the journal Frontiers in Earth Science

Received: *23 February 2022*
Accepted: *04 May 2022*
Published: *14 June 2022*

Citation:
Hu G, Guo J, Tian L, Wu X, Su J, Li Z and Fang C (2022) The Effect of Thermochemical Sulphate Reduction on the Carbon Isotope Ratio of Individual Light Hydrocarbons Associated With Natural Gas. Front. Earth Sci. 10:881762. doi: 10.3389/feart.2022.881762

INTRODUCTION

Table A1 Table Light hydrocarbons (LHs) associated with gas contain abundant geochemical information, so they have been widely used to determine the genetic type and origin of natural gas (Hu et al., 1990; Dai, 1993; Mango, 1997; Tassi et al., 2012; Hu et al., 2018). In particular, the iso/normal alkane ratio, normal heptane (nC_7), methylcyclohexane (MCH), and total dimethylcyclopentane (DMCP) ternary diagram are usually utilized to identify the type of organic source. Moreover, the nC_7 and isoheptane indices are often used to indicate maturity (Thompson, 1983). The ratios of iso-alkanes to n-alkanes (iC_5/nC_5, 3-MP/nC_6) have been applied to identify the extent of biodegradation (Welte et al., 1982; BeMent et al., 1995; George et al., 2002). Among isomers, these isotopic distributions are strong evidences indicating that the formation of these gasoline-range hydrocarbons is intricately linked to the isotopic signature of the precursor molecules from which they are derived (Whiticar and Snowdon, 1999). The carbon isotopes of individual LHs associated with natural gas are an effective tool for identifying the origin of natural gas. It mainly focuses on identifying coal-derived gas and oil-associated gas by using the carbon isotopic composition of benzene (BEN), toluene (TOL), CH and MCH (Jiang et al., 2000; Li et al., 2003; Dai et al., 2005; Hu et al., 2008). Jiang et al. (2000) have reported that the carbon isotopes of BEN and TOL in the LHs of natural gas are mainly influenced by the type of organic matter, while the thermal evolution and migration effect have only minor influence. In particular, Li et al. (2003) have argued that the carbon isotope of TOL is associated with the type of organic matter in the source rocks. Thus, the correlation of gas with the source rocks can be determined based on examination of the carbon isotopes of TOL in natural gas and source rocks. Hu et al. (2008) have analyzed the individual LHs isotope of abundant typical coal-derived/oil-associated gas samples from the Tarim and Ordos Basins in China and further proposed that the carbon isotopes of CH and MCH can be also utilized to identify coal-derived and oil-associated gases. The coal-derived gases with $\delta^{13}C_{CH}$ > -24‰ and $\delta^{13}C_{MCH}$ > -24‰, the oil-associated gases are opposite. Therefore, $\delta^{13}C_{CH}$ = -24‰ and $\delta^{13}C_{MCH}$ = -24‰ can be also used as cut-off plot to identify coal-derived gas and oil-associated gas.

The carbon isotopes of individual LHs are not only affected by the type of organic matter but also by secondary processes such as biodegradation and evaporation. During biodegradation, the straight chain is less abundant in ^{13}C than cycloalkanes and aromatics, whereas ^{12}C is preferentially consumed, thereby enriching each residual LH molecule in ^{13}C (George et al., 2002; Vieth and Wilkes, 2006). The $\delta^{13}C_{final\text{-}initial}$ of individual LHs in the C_6-C_8 range >1‰ mainly occurs when evaporative losses of individual LHs are >70%. However, nearly complete absence of stable carbon isotopic fractionation has been previously reported for cycloalkanes (Xiao et al., 2012). TSR, thermochemical sulphate reduction is the thermally driven reaction of sulphate (anhydrite) with hydrocarbon producing combinations of H_2S, carbonate minerals (e.g., calcite, $CaCO_3$), CO_2, elemental sulphur and water (Worden and Smalley, 1996). The TSR would preferentially consume the ^{12}C of C_5-C_8 individual LHs that are more enriched in ^{13}C, such as the $\delta^{13}C$ LHs of the crude oil, which increased up to 10‰ by TSR in the Western Canadian Sedimentary Basin. Isoalkanes, cycloalkanes and aromatics were more diagnostic for TSR and oil-source correlation than normal alkanes (Whiticar and Snowdon, 1999). Owing to the increasing H_2S concentration in carbonate gas reservoir was strongly associated with decreasing hydrocarbon content, Worden and Smalley (1996) used a gas souring index (GSI) to characterize the extent of TSR. Heavy hydrocarbon gas is preferentially consumed in the TSR process. Thus, the drying coefficient of natural gas affected by TSR is often reported to be high (Liu et al., 2013). Research on the carbon isotopes of individual hydrocarbons, associated with natural gas by TSR often focuses on low-molecular-weight gaseous hydrocarbons (C_1-C_4) (Hao et al., 2008). Thus far, only a few studies have used the carbon isotope ratios of LHs associated with gas as indicators of TSR. The gases from the TZ-I gas field in the Tarim Basin and the ZB gas field in the Sichuan Basin originated from marine source rocks and have been affected by TSR (Cai et al., 2001; Zhu et al., 2011; Cai et al., 2015).

This study evaluates the TSR process by using carbon isotope fractionation of LHs based on 15 gas-producing samples from TZ-I and ZB gas fields (Tarim and Sichuan Basin, China). To this end, the composition, stable carbon isotope of C_1 to C_4, quantification, and the individual compound-specific carbon isotopes of C_6-C_7 LHs were determined. The main objectives of this study are (a) to determine the molecular composition characteristics of C_1-C_4 and C_6-C_7 LHs for marine gas from the gas fields of TZ-I in the Tarim Basin and ZB in the Sichuan Basin; (b) to measure the individual compound-specific carbon isotopes of the C_1-C_4 and C_6-C_7 LHs; (c) to elucidate the genetic type, oil-cracking stage and TSR degree of the gases by the relative content, $\delta^{13}C$ of C_1-C_4 and LHs as well as GSI from these two gas fields (d) to examine the effect of TSR on the carbon isotopes of individual LHs.

TABLE A1 | The light hydrocarbon of C_6–C_7.

Compound	Abbreviation
2-methylpentane	2-MP
3-methylpentane	3-MP
normal-hexane	nC_6
methylcyclopentane	MCP
benzene	BEN
cyclohexane	CH
dimethylcyclopentane	DMCP
normal-heptane	nC_7
methylcyclohexane	MCH
toluene	TOL

GEOLOGICAL SETTING

The Tazhong area is an essential oil and gas exploration target in the Tarim Basin. The TZ-I gas field is located on the northern slope of the Tazhong Uplift in the Tarim Basin, between the central horst zone and Tazhong No. 1 fault zone, as shown in **Figure 1A**. The area of the field is ~264.54 km^2. It is the deepest

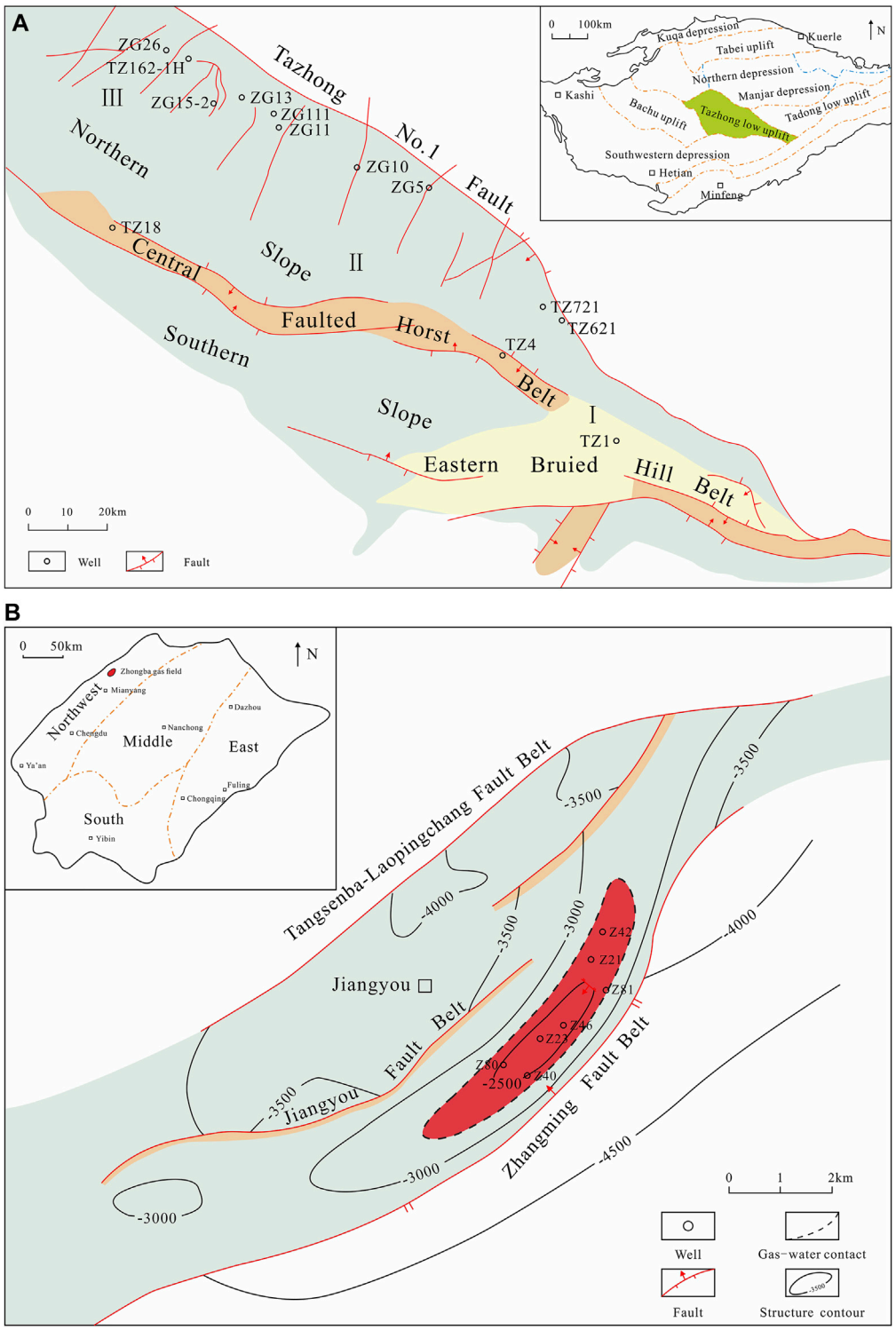

FIGURE 1 | Sketch maps showing the location of the TZ-I gas field in Tarim basin **(A)** (modified after Wu et al., 2014 and Guan et al., 2020) and ZB gas field in Sichuan basin **(B)** (modified from Zhu et al., 2011).

and oldest large reef-shoal complex condensate gas reservoir discovered in the Tarim Basin. The TZ-I gas field is divided into three zones ordered by the F82 and F14 horst zones. Zone I mainly represents a margin reef-bank condensate gas reservoir and buried hill dolomite condensate gas reservoir in the Lianglitage Formation platform. Zone II is mainly a fracture-

vuggy condensate gas reservoir in the Ordovician Lianglitage Formation and Yingshan Formation. At last, Zone III is the fracture-vuggy reservoir of the Yijianfang Formation (Guan et al., 2020). The buried depth of the three main Ordovician exploitation reservoirs ranges from 4,500 to 7,000 m, while the average buried depth exceeds 5,000 m. The height of the gas column and fluid distribution are controlled by the reservoir growth depth, rather than by the local structure and closure height, with a salient water body but no unified gas-water interface within (Wang et al., 2013; Zhou, 2013). The reservoir features various lithologies and hydrocarbon storage types. The former includes bioclastic, clastic, and reef limestones, and the latter embraces numerous modified pore holes, caves, and fissures. Moreover, the reservoir features physical properties with a porosity of 1.8%–4.1%, with an average of 2.3%, and permeability in the 0.01–452 md range (average estimate = 53 md) (Yang et al., 2007). The natural gas contains 17.5×10^4 to 18.4 $\times$ 10^4 mg/m^3 of hydrogen sulphide. The reservoir water belongs to the $CaCl_2$ type, with an average density and pH value of 1.09 g/cm^3 and 6.87, respectively. These phenomena confirmed good water preservation conditions and relatively weak groundwater activity. The Cambrian and lower Ordovician are composed of thick dolomites with intercalated dark mudstones and shales, which arguably represents the main source rocks (Cai et al., 2009). Besides, the ^{13}C of crude oil from Ordovician reservoir in TZ area (from −31.5‰ to −30.5‰) is consistent with the ^{13}C of kerogen from Cambrian source rock (−31.0‰ to −28.0‰), indicating that the condensate oil and gases derived from Cambrian and lower Ordovician source rocks. The TZ-I fault is an important conducting pathway for oil and gas (Zhao et al., 2009). It is located in the northern margin of the Tazhong low uplift and extends over 200 km. Also, it represents the boundary between the Tazhong low uplift and the Manjar Depression. The TZ-I fault is also the circulation channel of deep hydrothermal fluid with dissolution. The broken rock in the fracture zone receives bidirectional dissolution of atmospheric fresh water and deep hydrothermal fluid. Meanwhile, Karst fracture-vuggy reservoirs are distributed mostly along the strike-slip fault zone. The fault zone is the main factor, governing the fracture-vuggy carbonate reservoir.

The ZB gas field is a NE trending nose structure, located in a low anticline in the front fold belt of Longmen Mountain in the northwestern Sichuan Basin (**Figure 1B**) (Zhu et al., 2011). The gas field is composed of the Xuer gas reservoir of the Triassic Xujiahe Formation (T_3x^2) and Leisan gas reservoir of the Leikoupo Formation (T_2l^3). The Leikoupo Formation comprises a set of marine strata. The buried depth of the Leikoupo gas reservoir ranges from 3,140 to 3,510 m. It virtually represents a compound trap, composed of an anticline and fault-screened structure and a fracture-pore edge type water gas reservoir. The unified original gas-water interface altitude is -2,871 m, the gas-bearing area is 13.4 km^2, the gas-bearing height is 473 m, and the proven reserve is 86.3×10^8 m^3. The original formation pressure of the gas reservoir is 35.3 MPa, and the formation temperature is 86.1°C. The lithology of the reservoir is gray fine crystal dolomite, powdery crystal dolomite, algal debris, and sand debris dolomite of the Lower Leisan Formation. The acid insoluble matter content is <1%, and the thickness is ~100 m. The reservoir was stable in the transverse direction, and the average effective thickness of the gas reservoir was 74.2 m. The main type of storage and permeability space is represented by pinholes, with an effective porosity of 2%–4% (average = 5.4%). The permeability varies from 0.01 md to 35.04 md, and the average water saturation is 39.4%. Natural gas contains hydrogen sulphide and a high content of heavy hydrocarbons. Natural gas mainly originates from marine Cambrian or Permian sapropelic source rocks (Liao et al., 2014). The stable carbon isotope of condensate oil associated with gas from T_2l^3 in ZB gas field varied slightly from −31.5‰ to −31.8‰ also indicated the gases from type II kerogen. The Leikoupo Formation continued to descend and is buried deeply in the Lower Cretaceous, and the maximum thickness of the residual strata of the Lower Cretaceous in northwest Sichuan reached over 1,700 m. It has been previously estimated that the buried depth of the Leisan reservoir in the ZB gas field is >4,000 m, and the paleogeothermal temperature is >200°C. During the deep burial process, which lasted ~70–80 million years from the Early Cretaceous to Tertiary, crude oil was thermally cracked into natural gas. Some of the pores of the Leisan algae sand-debris pinhole dolomite are filled with black and brown bitumen, thereby, physically suggesting petroleum cracking. Given the high temperature, driven by deep burial, the anhydrite contained in the Leikoupo Formation dissolved in the formation water and produced sulphate, which reacted with hydrocarbon gas in the gas reservoir to produce hydrogen sulphide (the sulfuric acid content in the formation water of the Zhongba Leisan strata reached 712–1,109 g/L). Consequently, the hydrogen sulphide content in Zhongba Leisan gas reservoir is as high as 4.95%–8.34%. On one hand, the structural deformation of Zhongba in the late Himalayan period exacerbated the fractures of the reservoir, which was conducive to the seepage of natural gas and obtaining high-production gas wells. On the other hand, the structural trap area and closure were dwindled, fluid potential energy was changed, gas-water interface was adjusted, part of natural gas was lost, and the other part of natural gas reacted with formation water sulphate to generate hydrogen sulphide under the action of thermal catalysis. Moreover, the content of hydrocarbon gas was weakened, and the gas reservoir was somehow damaged.

SAMPLING AND ANALYTIC METHODS

Sampling

Fifteen gas samples were collected at the wellheads of commercial gas production wells using 15 stainless steel cylinders with double valves. First, the cylinder was flushed for 15–20 min to remove air contamination. Second, eight gases were sampled from the TZ-I gas field and seven gases were sampled from the ZB gas field. Note that the pressure inside the cylinder was kept as high as 1–5 MPa.

Analytic Methods

Gas composition, carbon isotope of C_1-C_4 and CO_2, as well as chemical and isotopic compositions of the LHs were analysed. All

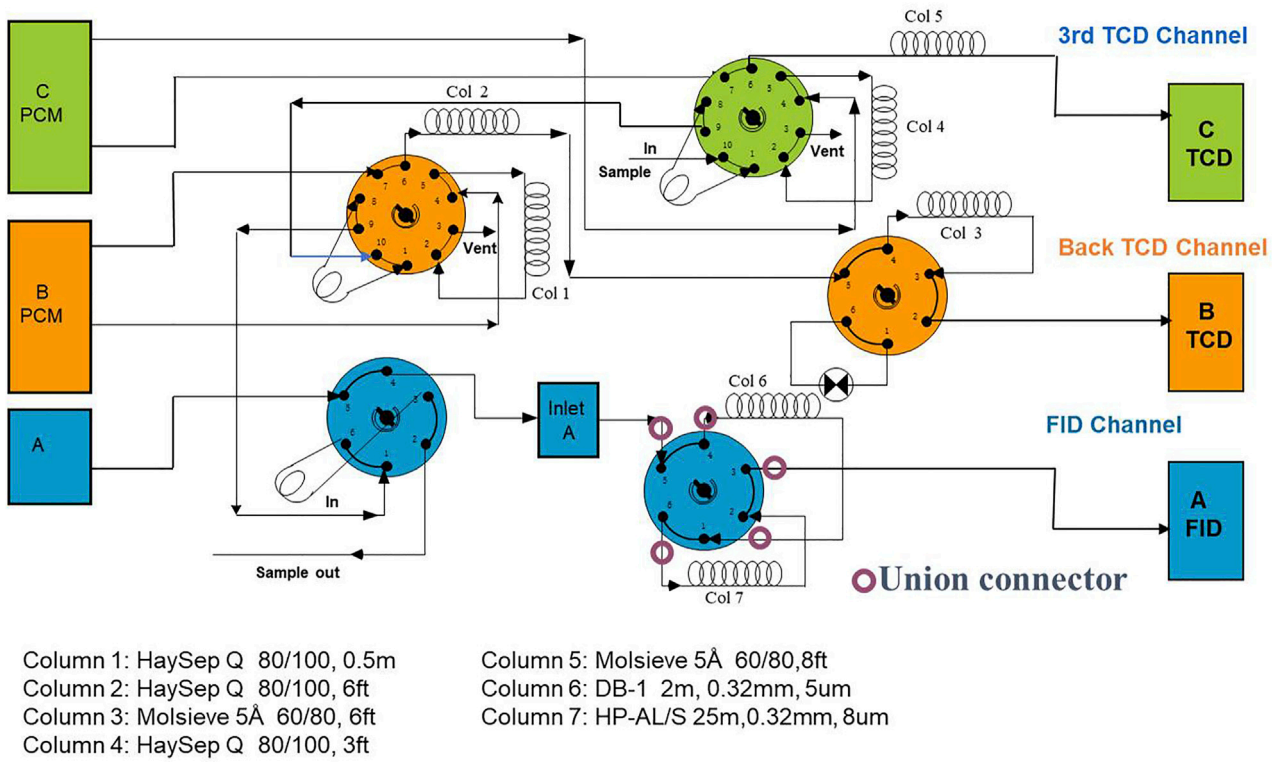

FIGURE 2 | Configuration of Agilent 7890B gas chromatograph (GC) with 5 valves, 7 columns and 3 detectors for analyzing hydrocarbon and non-hydrocarbon components of natural gas.

the sample preparation and measurements were finished in the Key Laboratory of Petroleum Geochemistry at the Research Institute of Petroleum Exploration and Development of PetroChina. The individual hydrocarbon and non-hydrocarbon components of natural gas were identified and quantified using an Agilent 7890B gas chromatograph (GC), equipped with a flame ionisation detector (FID), and two thermal conductivity detectors (TCD). The configuration of Agilent 7890B as shown in **Figure 2**. Helium was used as the carrier gas for the FID and the first TCD. The proportion of N_2, CO_2, and H_2S was detected by the first TCD, and the second TCD only measured the proportion of He which was carried by nitrogen as the carrier gas. All the carrier gas were high purity He (99.9995%) and N_2 (99.9999%). The inlet temperature was set at 150°C. The initial oven temperature was initially set at 35°C for 5 min, then programmed to 100°C at 10°C/min, and finally to 200°C at 20°C/min. The external standard gases indicated the GC had a precision of better than ±0.3 mol% for each component.

Carbon isotopic compositions of the gases were analysed using a Thermo Delta V mass spectrometry interfaced to a Thermo gas chromatograph *via* a combustion interface. Individual gaseous hydrocarbon compounds were separated using a PQ capillary column. Temperatures of the inlet and the oxidation oven were set at 200°C and 980°C, respectively. The gas chromatograph temperature started at 33°C and was kept steady for 5 min, then programmed to rise from 33°C to 80°C at 8°C/min, from 80 to 170°C at 5°C/min, and finally from 170°C to 250°C at 6°C/min. Every sample was analysed at least twice. The stable carbon isotopic values are reported in the δ-notation in per mil (‰) relative to the Vienna Peedee Belemnite standard (VPDB), and the reproducibility for $\delta^{13}C$ measurement is ±0.5‰. The calibrated standard values of the oil-derived gas in ‰ relative to VPDB in our laboratory are $\delta^{13}C_1 = -43.61 \pm 0.09‰$, $\delta^{13}C_2 = -40.24 \pm 0.10‰$ and $\delta^{13}C_3 = -33.79 \pm 0.09‰$. The assigned values are fundamentally traceable to the international carbon isotope standard of VPDB (Dai et al., 2012).

Furthermore, LHs were analysed on a HP5890A gas chromatography with a PONA capillary column. The components were collected with a liquid nitrogen cold trap for 10 min, and the eluting hydrocarbons were detected using a FID at 300°C. The initial oven temperature was maintained at 30°C for 15 min, ramped up to 70°C at a rate of 1.5°C/min and then to 280°C at 2.5°C/min. The standard test mixture contained 53 compounds (i-butane to normal octane). Note that the LH analysis of the test mixture was performed before the analysis of the study samples to ensure the sample analysis quality and comparability of analytical samples at different time periods.

The carbon isotopic compositions of the individual LHs were determined *via* gas chromatography–combustion-isotope ratio monitoring mass spectrometry by freezing the GC column in a cold trap filled with liquid nitrogen. Note that precise and explicit analytical methods were introduced in details in Hu and Zhang (2011). The Thermo Trace GC Ultra gas chromatograph connected to MAT 253 isotopic mass spectrometer (Thermo

TABLE 1 | The molecular composition and stable carbon isotope of natural gas from the TZ- I and ZB gas fields.

Gas fields	Well	Strata	Depth/m	Composition/%												$\delta^{13}C$/‰, VPDB			
				CH_4	C_2H_6	C_3H_8	*i*-C_4	*n*-C_4	C_1-C_4	Dryness	N_2	CO_2	He	H_2S	GSI	CH_4	C_2H_6	C_3H_8	CO_2
TZ-I	ZG162-1H	O_I	6,094.83–6,780	85.3	4.1	1.6	0.4	0.7	92.0	0.93	4.6	3.3	0.04	0.1	0.12	-47.3	-36.4	-30.8	-2.2
	ZG26	O_{II}	6,085.5–6,295	77.7	4.2	5.2	1.7	1.9	90.7	0.86	5.9	3.3	0.05	0.0	0.02	-49.0	-37.0	-32.5	-1.8
	ZG15-2	O_I	5,918.5–6,155	76.4	8.6	4.3	1.0	1.7	91.9	0.83	6.3	1.7	0.04	0.1	0.13	-51.5	-38.4	-32.2	n.d.
	ZG13	O_{II}	6,458–65,504	75.5	10.4	5.2	1.1	2.4	94.5	0.80	1.2	4.2	0.03	0.1	0.12	-49.9	-37.0	-32.0	-5.2
	ZG111	O_{II}	6,008–6,250	88.2	4.4	1.7	0.5	0.7	95.5	0.92	1.7	2.4	0.04	0.4	0.46	-46.7	-33.0	-29.6	n.d.
	ZG11	O_{II}	6,165–6,631.1	89.4	3.6	1.4	0.4	0.7	95.6	0.94	1.9	1.7	0.04	0.8	0.83	-47.5	-35.6	-28.5	-11.9
	TZ721	O_I	5,355.5–5,505	93.8	0.5	0.2	0.0	0.1	94.7	0.99	0.9	4.4	0.04	0.0	0.01	-42.1	-35.6	-31.0	n.d.
	TZ621	O_I	4,851–4,885	91.1	1.7	0.7	0.2	0.3	94.0	0.97	3.4	2.6	0.04	0.0	0.04	-38.2	-34.1	-31.7	-3.0
		Average		84.7	4.7	2.5	0.7	1.1	93.6	0.90	3.2	2.9	0.04	0.2	0.22	-46.5	-35.9	-31.0	-4.8
ZB	Z46	T_2^3	3,134.51	83.4	1.6	0.5	0.1	0.3	85.9	0.97	1.7	5.1	0.04	7.2	7.72	-34.2	-29.3	-27.5	-4.9
	Z40	T_2^3	3,121.7	82.7	1.5	0.5	0.1	0.2	85.1	0.97	2.0	5.2	0.04	7.6	8.21	-34.5	-28.1	-26.9	-4.6
	Z42	T_2^3	3,358.75	82.5	1.6	0.6	0.2	0.3	85.2	0.97	1.6	5.4	0.06	7.7	8.28	-33.5	-28.2	-27.0	-4.4
	Z80	T_2^3	3,120	83.0	1.6	0.5	0.2	0.3	85.4	0.97	2.5	4.2	0.05	7.8	8.35	-34.4	-28.4	-28.6	-5.4
	Z81	T_2^3	3,231.7	84.4	1.4	0.4	0.1	0.2	86.6	0.97	1.5	4.9	0.04	7.0	7.45	-34.2	-28.6	-26.8	-4.6
	Z21	T_2^3	3,303	82.2	1.6	0.5	0.2	0.3	84.8	0.97	2.5	4.9	0.06	7.8	8.45	-33.7	-28.0	-26.5	-4.1
	Z23	T_2^3	3,100	83.3	1.6	0.5	0.1	0.3	85.9	0.97	2.3	4.5	0.04	7.3	7.86	-35.1	-28.0	-26.7	-3.9
		Average		83.1	1.6	0.5	0.2	0.3	85.6	0.97	2.0	4.9	0.05	7.5	8.04	-34.2	-28.4	-27.1	-4.6

n.d., not detected.

Fischer Scientific) *via* a micro-combustion furnace and water-removal assembly. The carrier gas was helium, and the inlet temperature was 200°C. The amount of sample injected is 1–10 ml, and the components were collected with cold trap for 5 min. The initial oven temperature was held at 30°C for 15 min and then programmed to 70°C at 1.5°C/min, then rose from 70°C to 160°C at 3°C/min, finally from 160°C to 250°C at 5 °C/min. The final temperature was held for 20 min. A mixture of standards of n-alkanes from A. Schimmelmann of Indiana University was measured two times before sample testing. Every sample was analysed at least twice. The stable carbon isotopic values were calibrated relative to the PeeDee Belemnite Standard (V-PDB) with an error of less than 0.5‰.

RESULTS

Molecular Composition of Natural Gas

The molecular compositions of the gases from the TZ-I and ZB gas fields are shown in **Table 1**. All the natural gases were dominated by methane, ranging from 75.5% to 93.8% (average = 83.9%). The total contents of C_1-C_4 alkane gases ranged from 84.8% to 95.6% (average = 89.8%). However, some remarkable differences of the alkane gas compositions in the TZ-I and ZB gas fields were identified. The contents of all alkane gases in the TZ-I gas field were higher than those in the ZB gas field. The content in the TZ-I gas field ranged from 90.7% to 95.6% (average = 93.6%) and from 84.8% to 86.6% (average = 85.6%) in the ZB gas field. The gas dryness coefficient, defined as $C_1/(C_1$-$C_4)$, exhibited strong variations (0.80–0.99) with the averages of 0.90 and 0.97 for TZ-I and ZB gas fields, respectively (**Table 1**). The alkane gas composition in the TZ-I gas field strongly with the content of methane from 75.5% to 93.8% and mostly wet gases, $C_1/(C_1$-$C_4) < 0.95$, except the wells TZ621 and TZ721 (**Figure 3A**). The gases in the ZB gas field slightly varied with the concentration of methane from 82.2% to 84.4% and were found to be very dry (the dryness coefficient = ~0.97).

The content of non-hydrocarbon gases exhibited strong variability (4.4%–15.2%) except for noble gas, helium. Notably, greater differences were identified between the gases in the TZ-I and ZB gas fields (**Figure 3B**). In general, non-hydrocarbon gas exhibits high concentration in the ZB gas field, compared with that in the TZ-I gas field. The gas in the TZ-I gas field was mainly composed of N_2 (3.2% on average) and CO_2 (2.9%), while the H_2S contents were extremely low from 0.01% to 0.80%, regardless of the content variation of methane. Meanwhile, in the ZB gas field, the H_2S content was found to be fairly homogeneous, from 7.0% to 7.8%, and the highest (7.5% on average) among non-hydrocarbon gases, followed by CO_2 (4.9% on average) and N_2 (2.0% on average). Besides, the gas souring index (GSI) in the ZB gas field (from 7.45 to 8.45 with an average of 8.04) is greater than that in the TZ-I gas field (from 0.01 to 0.83 with a mean of 0.22).

Carbon Isotope of Gaseous Alkanes

The carbon isotopic compositions of the individual components of the gases in the TZ-I and ZB gas fields are listed in **Table 1**. The

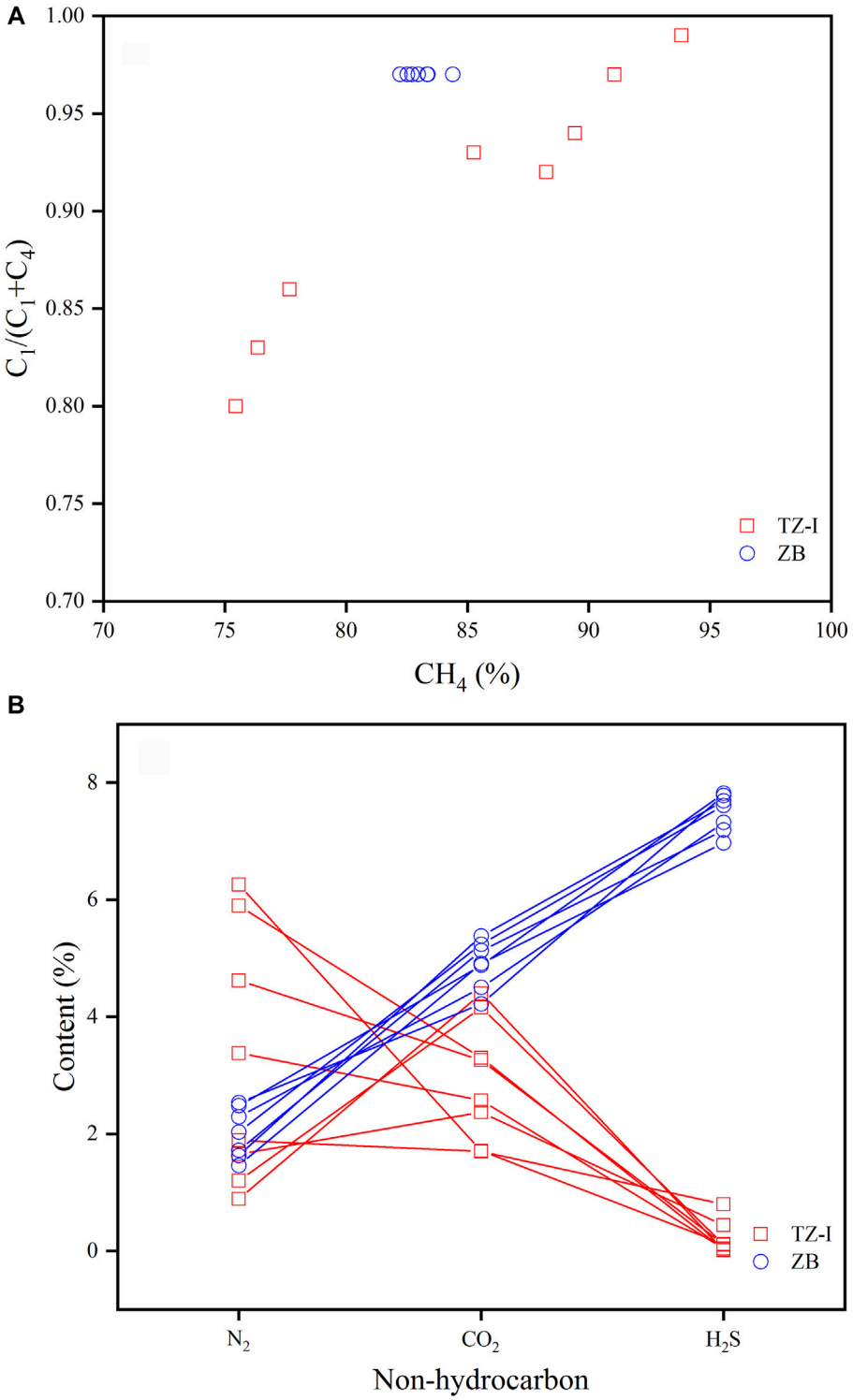

FIGURE 3 | The correlation of $C_1/C_{1\text{-}4}$-CH_4% **(A)** and N_2%-CO_2%-H_2S% **(B)** of natural gases in the TZ-I and ZB gas fields.

methane carbon isotope composition ranged from −51.5‰ to −33.5‰ (average = −40.8‰). The $\delta^{13}C$ value of ethane ranged from −38.4‰ to −28.0‰ (average = −32.4‰), and that of propane ($\delta^{13}C_3$) ranged from −32.5‰ to −26.5‰. **Figure 3** shows that all the gas samples exhibited a normal stable carbon isotope trend for C_1–C_3 alkanes ($\delta^{13}C_1 < \delta^{13}C_2 < \delta^{13}C_3$). However, the carbon isotopes of the natural gas components in the two gas fields significantly varied (**Table 1**;

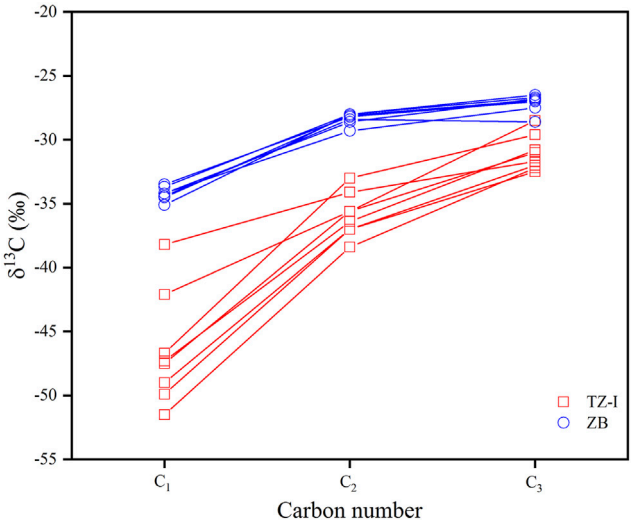

FIGURE 4 | Relationship between $\delta^{13}C$ and carbon number of gases in the TZ-I gas field and the ZB gas field.

Figure 4). The carbon isotopes of the natural gas components in the TZ-I gas field were found to be very light. In particular, the $\delta^{13}C_1$ ranged from −51.5‰ to −38.2‰ (average = −46.5‰), $\delta^{13}C_2$ ranged from -38.4‰ to -33.0‰ (average = −35.9‰), and $\delta^{13}C_3$ ranged from −32.5‰ to −28.5‰ (average = -31.0‰). The carbon isotopes of natural gas components in the ZB gas field were relatively heavy, whereas $\delta^{13}C_1$ ranged from −35.1‰ to −33.5‰ (average = -34.2‰), $\delta^{13}C_2$ ranged from −29.3‰ to −28.0‰ (average = −28.4‰), and $\delta^{13}C_3$ ranged from −28.6‰ to −26.5‰ (average = −27.1‰). The $\delta^{13}C_1$, $\delta^{13}C_2$, $\delta^{13}C_3$ values in the ZB gas field exceeded 12.3‰, 7.5‰, and 3.9‰, respectively, compared to those in the TZ-I gas field. The CO_2 carbon isotope in some samples was also measured. It was found that the $\delta^{13}C$ values ranged from -11.9‰ to −1.8‰, thereby indicating that the carbon isotope variation of CO_2 in the two gas fields was very high. The $\delta^{13}C_{CO2}$ in the TZ gas field widely ranged from −11.9‰ to −1.8‰, whereas in the ZB gas field presented a slightly vary from −5.4‰ to −3.9‰.

Molecular Variability of C_6-C_7 LHs

The molecular variability of the C_6-C_7 LHs, associated with the gases in the TZ-I and ZB gas fields is shown in **Table 2** and **Figures 6A,B**. The gases in the two gas fields were notably characterized by the high content of normal and isoalkanes. Among the C_6-C_7 compounds, the relative contents of normal and isoalkanes ranged from 60.5% to 85.9% (average = 71.6%) higher than that of cycloalkanes and aromatics, respectively (**Table 2**). Meanwhile, the concentration of normal and isoalkanes in the ZB gas fields was lower than TZ-I gas field, about 10% (**Figure 6A**). The content of nC_7 was found to be highest among nC_7, DMCP, and MCH, it ranged from 44.1% to 70.5% (average = 54.6%). However, the abundance of DMCP and MCH were somewhat low, with the average estimates of 15.4% and 30.0%, respectively. Furthermore, there were some differences in the compositions of nC_7, DMCP, and MCH compounds. Specifically, the relative nC_7 content in the TZ-I gas field was significantly higher than that in the ZB gas field (**Figure 6B**). In contrast, the relative contents of DMCP and MCH in the ZB gas field were higher than those of the TZ-I field.

Isotope Variability

The compound-specific carbon isotopic compositions of the C_6-C_7 hydrocarbons of the 15 gas samples measured to examine their isotopic characteristics, the response to TSR and origin. Given the co-elution or insufficient partition of adjacent hydrocarbon components and low abundance, only nine compounds were analysed from isotope ratio perspective. The carbon isotope compositions of the nine compounds of the various samples

TABLE 2 | The relative contents of C_6-C_7 light hydrocarbons of natural gases from the TZ-I and ZB gas fields.

Gas fields	Well	Strata	Depth/m	C_6-C_7/GC area, %					C_7/GC area, %		
				Normal alkane	Isoalkane	Normal and isoalkanes	Cycloalkane	Aromatic	Heptane	Dimethyl cyclopentane	Methyl cyclohexane
TZ-I	ZG162-1H	O_{II}	6,094.83–6,780	45.9	32.5	78.5	13.7	7.8	70.5	8.3	21.2
	ZG26	O_{III}	6,085.5–6,295	41.1	38.4	79.5	15.1	5.4	67.7	8.9	23.4
	ZG15-2	O_{II}	5,918.5–6,155	40.5	39.3	79.8	14.6	5.6	64.2	12.9	22.9
	ZG13	O_{III}	6,458–6,550.36	38.3	47.6	85.9	10.8	3.3	58.2	21.3	20.5
	ZG111	O_{III}	6,008–6,250	41.2	33.9	75.1	18.0	6.9	65.3	9.2	25.6
	ZG11	O_{III}	6,165–6,631.1	39.0	34.0	72.9	19.2	7.9	57.8	12.6	29.6
	TZ721	O_I	5,355.5–5,505	37.3	32.8	70.1	17.0	12.9	60.7	13.2	26.1
	TZ621	O_I	4,851–4,885	38.2	35.9	74.2	18.1	7.7	59.4	14.3	26.3
		Average		40.2	36.8	77.0	15.8	7.2	63.0	12.6	24.4
ZB	Z46	T_2l^3	3,134.5	31.4	35.1	66.5	22.3	11.2	46.6	18.8	34.6
	Z40	T_2l^3	3,121.7	32.2	38.8	71.0	16.8	12.2	44.3	22.1	33.6
	Z42	T_2l^3	3,358.8	32.9	39.0	71.9	20.4	7.7	44.6	20.8	34.6
	Z80	T_2l^3	3,120	31.8	32.4	64.2	25.1	10.7	45.6	17.8	36.6
	Z81	T_2l^3	3,231.7	30.6	30.5	61.1	25.8	13.1	44.1	16.6	39.3
	Z21	T_2l^3	3,303	31.2	31.6	62.7	25.6	11.7	44.6	17.4	38.1
	Z23	T_2l^3	3,100	29.6	30.9	60.5	25.2	14.3	45.0	17.0	38.0
		Average		31.4	34.0	65.4	23.0	11.5	45.0	18.6	36.4

TABLE 3 | Individual light hydrocarbons carbon isotope of fifteen gases from the TZ-I and ZB gas fields.

Gas fields	Well	Strata	Depth/m	$\delta^{13}C$‰(VPDB)								
				2-MP	3-MP	nC_6	MCP	BEN	CH	nC_7	MCH	TOL
TZ-I	ZG162-1H	O_{II}	6,094.83–6,780	-28.8	-29.0	-29.4	-28.0	-28.1	*-29.5*	-30.1	-31.0	-28.5
	ZG26	O_{III}	6,085.5–6,295	-29.6	-29.6	-30.9	-29.7	-29.1	*-30.2*	-30.7	-31.5	-30.1
	ZG15-2	O_{II}	5,918.5–6,155	-28.9	-28.9	-29.8	-28.6	-29.3	*-31.0*	-30.9	-31.5	-29.5
	ZG13	O_{III}	6,458–6,550.36	-28.6	-29.4	-30.3	-30.0	-28.1	*-30.8*	-30.3	-32.3	-29.6
	ZG111	O_{III}	6,008–6,250	-28.4	-29.8	-29.5	-30.9	-29.0	*-31.9*	-30.9	-32.6	-30.5
	ZG11	O_{III}	6,165–6,631.1	-27.8	-28.4	-28.7	-29.1	-27.7	*-29.2*	-29.9	-29.8	-28.5
	TZ721	O_I	5,355.5–5,505	-28.1	-28.6	n.d.	-30.1	-28.6	*-29.0*	-30.2	-30.6	-30.0
	TZ621	O_I	4,851–4,885	-28.5	-28.9	-30.5	-28.7	-26.8	*-30.1*	-30.8	-32.3	-28.1
		Average		-28.6	-29.1	-29.9	-29.4	-28.3	*-30.2*	-30.5	-31.5	-29.4
ZB	Z46	T_2l^3	3,134.5	-28.3	-28.6	-27.8	-26.6	-27.9	*-27.2*	-30.8	-27.4	-28.1
	Z40	T_2l^3	3,121.7	-29.1	-28.7	-28.2	-27.0	-28.1	*-28.8*	-30.1	-28.1	-28.2
	Z42	T_2l^3	3,358.8	-27.5	-28.1	n.d.	-27.0	-27.9	-27.4	-30.5	-28.0	-28.0
	Z80	T_2l^3	3,120	-28.1	-28.0	-26.7	-26.5	-27.4	-27.6	-30.1	-28.0	-28.1
	Z81	T_2l^3	3,231.7	-28.8	-28.4	-25.8	-26.6	-27.8	-27.8	-30.2	-28.2	-28.2
	Z21	T_2l^3	3,303	-28.2	-28.7	n.d.	-27.8	-28.0	-28.4	-29.8	-29.0	-28.3
	Z23	T_2l^3	3,100	-28.9	-30.0	-28.7	-28.2	-27.0	-28.0	-28.4	-27.5	-28.0
		Average		-28.4	-28.6	-27.4	-27.1	-27.7	-27.9	-30.0	-28.0	-28.1

n.d., not detected.

are listed in **Table 3**. Despite slight offsets of single compounds between the different samples, all the compounds were generally enriched in ^{12}C. The carbon isotopes of branched alkanes 2-MP, 3-MP, nC_6, and nC_7 were relatively light. They ranged from −29.6‰ to −27.5‰, −30.0‰ to −28.0‰, −30.9‰ to −5.8‰ and −30.9‰ to −28.4‰, respectively. The carbon isotopes of cycloalkanes, such as MCP, CH, and MCH, somewhat differed in the two gas fields. Their carbon isotopes were relatively light in the TZ-I gas field with the average estimates of −29.4‰, −30.2‰, and −31.5‰, respectively. Meanwhile, the average values of the ZB gas field were −27.1‰, −27.9‰, and −28.0‰, respectively. The average difference was more significant than 2‰, while the difference in carbon isotopes of light aromatic BEN and TOL was rather minor. Specifically, the average values of carbon isotopes of BEN were found to be −28.3‰ and −27.7‰ in the TZ-I and ZB gas fields, respectively with only 0.6‰ differences. However, the differences were identified in the carbon isotopes of TOL; in average, the TZ-I gas field was 1.3‰ lighter than the ZB gas field.

DISCUSSION

Genetic Type of Gases

The molecular and isotopic variability of the C_1-C_4 and C_6-C_7 LHs can indicate the genetic type (oil-associated or coal-derived, primary cracking, or secondary cracking) of natural gas (Stahl and Carey, 1975; Dai et al., 2005; Hu et al., 2008). Bernard et al. (1978) have already utilized the $C_1/(C_2+C_3)$ ratio and $\delta^{13}C$ of methane (Bernard diagram) to elucidate the origin and possible process of gas generation. The $\delta^{13}C_1$ versus $\delta^{13}C_2$ cross plot is typically used to classify the origin and maturity trends of natural gas (Jenden et al., 1988; Rooney et al., 1995; Berner and Faber, 1996; Tilley and Muehlenbachs, 2013). Numerous empirical studies of gas carbon isotope geochemistry, conducted in the Chinese sedimentary basins, have suggested a threshold of $\delta^{13}C_2$ (−28‰) can be used to differentiate the origin of thermogenic gases. Generally, thermogenic gases, generated from sapropelic source rocks (oil-associated gas) are characterised by $\delta^{13}C_2$ values lighter than −28‰, whereas ethane and propane derived from humic source rocks (coal-derived gas) own carbon isotopic values heavier than -28‰ (Dai et al., 1992, Liang, et al., 2002; Dai et al., 2005; Xiao et al., 2008). The majority of the gases were plotted in the lower area of the cross plot of $\delta^{13}C_1$ vs. $\delta^{13}C_2$, $\delta^{13}C_2 < -28$‰, whereas the gases from the TZ-I gas field exhibited relatively lighter $\delta^{13}C_2$ values than those from ZB gas field (**Figure 5**). The difference between the two gas fields coincided with oil-associated gas or type II kerogen maturity trends (Jenden et al., 1988; Rooney et al., 1995; Tilley and Muehlenbachs, 2013). Therefore, we suggested that the heavier $\delta^{13}C_2$ of ZB gas field may be caused by the increasing process of thermal. Although some of the $\delta^{13}C_2$ of the gas originated from type III kerogen was < −28‰, methane, ethane, and propane carbon isotope distributions in these gases exhibited negative carbon isotope characteristics ($\delta^{13}C_1 > \delta^{13}C_2 > \delta^{13}C_3$) and were distributed in the over-mature area of source rocks (Dai et al., 2016). Different with the unusual gases, the carbon isotopes of the natural gas in the TZ-I and ZB gas fields were relatively light and presented a positive sequence distribution (**Figure 4**). This finding indicates that the natural gas in the TZ-I and ZB gas fields was derived from the Type II kerogen and not from the Type III kerogen in the over-mature stage.

The molecular composition and isotopic ratio of C_6-C_7 LHs can unravel the genetic type and source of natural gas. The ternary diagram of nC_7, DMCP, and MCH is also useful for distinguishing coal-derived gases from oil-associated gases (Hu et al., 1990; Dai, 1993; Hu et al., 2008). Hu et al. (2008) have already proposed that coal-derived gas typically contains >50% MCH among nC_7, DMCP, and MCH. The ternary composition

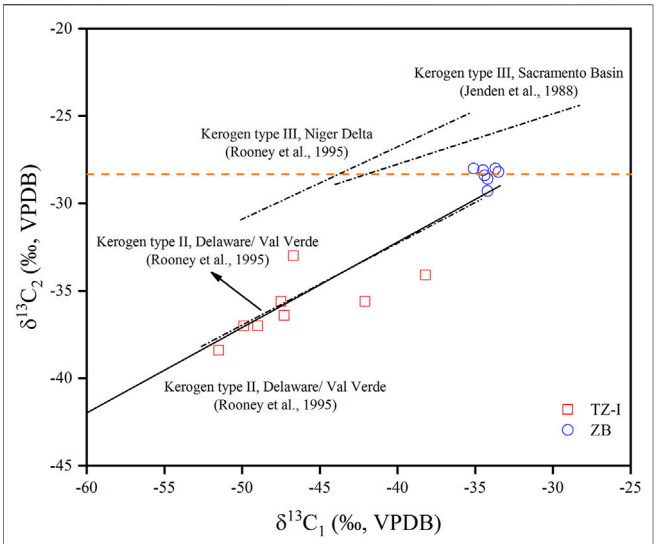

FIGURE 5 | $\delta^{13}C_1$ verse $\delta^{13}C_2$ cross plot of natural gases from TZ-I and ZB gas fields. Also shown are the maturity trend of type II kerogen (Rooney et al., 1995; Tilley and Muehlenbachs, 2013) and type III kerogen (Jenden et al., 1988; Rooney et al., 1995).

diagram of C_6-C_7 n-alkanes, isoalkanes, and cycloalkanes can be also widely used to identify the origin of natural gas (Hu et al., 2008). The relative content of C_6-C_7 normal and isoalkanes in the oil-associated gas was >30%, coal-derived gas was opposite. As shown in **Figure 6A**, the gases from the TZ-I and ZB gas fields were located in the area of oil-associated gas. In the ternary diagram of nC_7, DMCP and MCH, all of the gases from the TZ-I and ZB gas fields were also located in oil-associated gas areas (**Figure 6B**), thereby suggesting that these gases originated from the type II kerogen. Stable carbon isotope information, carried by the LHs, associated with oils and gas can be applied to elucidate the secondary alteration, origin, and correlation of oil and gas (Rooney et al., 1995; Whiticar and Snowdon, 1999; George et al., 2002; Li et al., 2003; Dai et al., 2005; Hu et al., 2008). Jiang et al. (2000) have already argued that the carbon isotopes of BEN and TOL are mainly affected by the type of organic matter, rather by thermal evolution and migration. Hence, the isotope ratio of light aromatic compound can be used to reflect the type of organic matter. Hu et al. (2008) have proposed the identification index of coal-derived gas and oil-associated gas by studying the carbon isotopes of BEN, TOL, CH, and MCH in light hydrocarbon from typical sedimentary basins in China. Generally, the carbon isotopes of BEN, TOL, CH, and MCH in the coal-derived gas are heavier. Specifically, $\delta^{13}C_{BEN}$ = −23‰, $\delta^{13}C_{TOL}$ = −24‰, $\delta^{13}C_{CH}$ = −24‰, and $\delta^{13}C_{MCH}$ = −24‰ can be used as cut-off points for the identification of oil-associated gas and coal-derived gas. As shown in **Figures 7A,B**, the gases from the TZ-I and ZB gas fields were located in the area of oil-associated gas, thereby indicating that these gases were sourced from type II kerogen.

The molecular components and individual carbon isotopes of C_1-C_4 and LHs demonstrated that the gases from TZ-I gas field in Tarim Basin and ZB gas field in Sichuan Basin sourced from sapropelic source rocks or type II kerogen. Our findings are consistent with the results of Wu et al. (2014) and Liao et al. (2014) on the gas genetic types.

Stage of Oil Cracking Gas

The generation of oil-associated gas by sapropelic organic matter can be further divided into kerogen cracking (primary cracking) gas and oil cracking (secondary cracking) gas. Numerous geochemistry studies aimed to distinguish between these two gases which generated from the thermal degradation (Behar et al., 1992; Prinzhofer and Huc, 1995; Lorant et al., 1998; Prinzhofer and Rocha (2000)). The chemical composition and stable carbon isotope characteristics of natural gas indicated that kerogen cracking gas and oil cracking gas can be identified. The cracking experiments, conducted by Hill et al. (2003) have already indicated that oil cracking gas in a closed system exhibited a low dryness index and $\delta^{13}C_1$ value. At a similar pyrolysis temperature, the $\delta^{13}C_1$ value of the kerogern cracking gas was heavier than that of the oil cracking gas due to the differences of precursors (Tian et al., 2007). Behar et al. (1992) have demonstrated that the C_1/C_2 and C_2/C_3 ratios followed different variation trends in the process of kerogen cracking and oil cracking. On this basis, the different variation tendencies in the ln (C_1/C_2)–ln (C_2/C_3) plot can be used to identify kerogen cracking and oil cracking gases (Prinzhofer and Huc, 1995). However, these parameters are not applicable for TZ gas fields (Wu et al., 2014). Lorant et al. (1998) and Prinzhofer et al. (2010) further suggested a quantitative ($\delta^{13}C_2$-$\delta^{13}C_3$) -(C_2/C_3) plot to classify kerogen cracking and oil cracking gases. Note that the gases from the TZ-I and ZB gas fields are barely located in the area of the primary cracking except minor samples (**Figure 8**). Tian et al. (2007) have reported that as the pyrolysis temperature increased, the $\delta^{13}C_1$ values of oil cracking gases decreased in the early cracking stage and then increased. The $\delta^{13}C_2$-$\delta^{13}C_3$ values of the gases in the TZ-I gas field ranged from −7.1‰ to −3.4‰, and the carbon isotopes of ethane (average = −35.9‰) and propane (average = −31.0‰) are very light. Furthermore, the C_2/C_3 values were relatively small, ranging from 0.81 to 2.64, although there were a certain amount of C_2 and C_3 (**Table 1**). This indicates that the gases in the TZ-I gas field were the early product of the secondary cracking of oil. **Figure 8** shows that the gases of ZB gas field are in the transition zone between the NSO compounds and crude oil cracking gas due to the smaller values of $\delta^{13}C_2$-$\delta^{13}C_3$ (from -1.8‰ to 1.2‰) compared to the TZ-I gas field. However, the gases in this gas field were drier with extremely low concentration of C_{2+} and more enrich ^{13}C in methane, demonstrating the maturity of the natural gas was higher than of the TZ-I gas field. The quite homogeneous heavier carbon isotope of ethane and propane also suggest that the gases undergo similar high thermal evolution. Therefore, it is reasonable to suggest that the natural gas in the ZB gas field may have mainly originated from the late cracking of oil or secondary cracking of wet gas rather than the NSO. Generally,

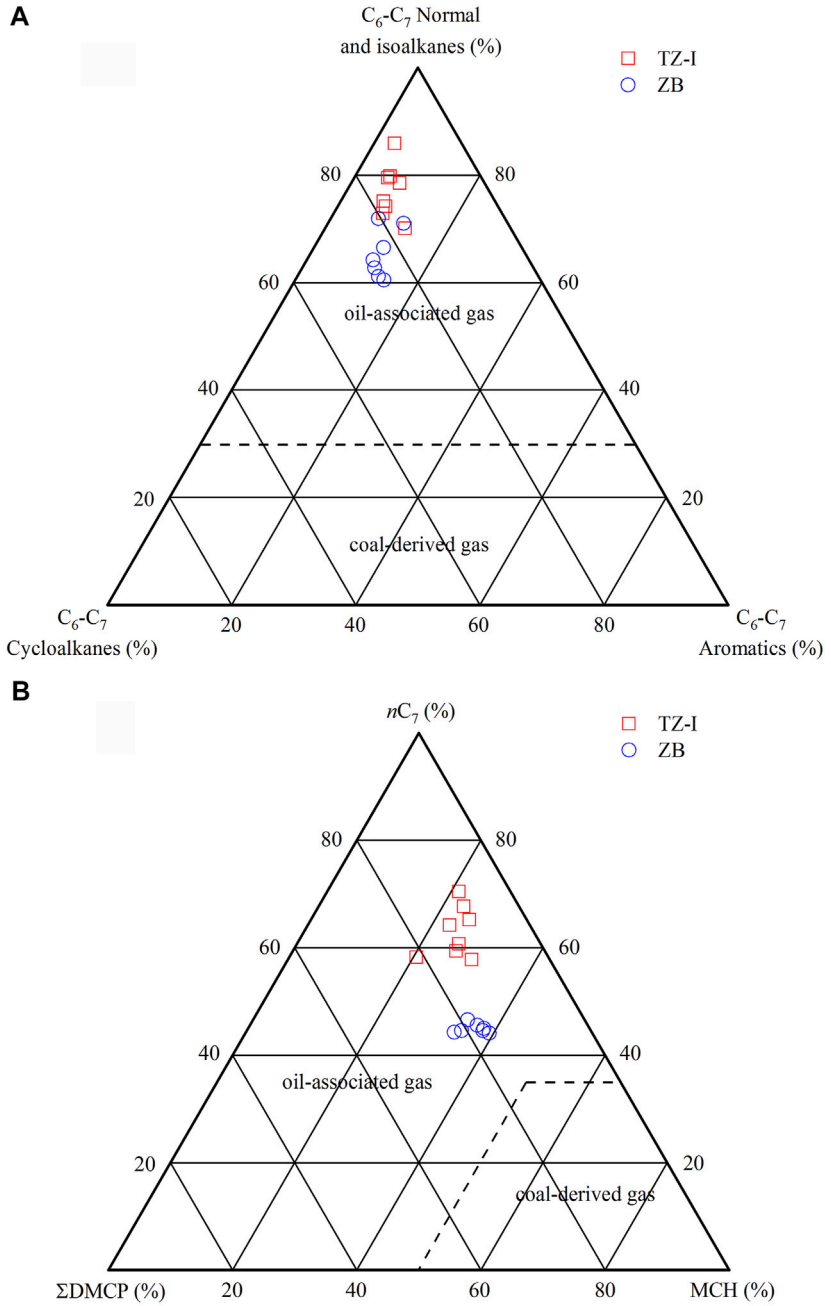

FIGURE 6 | Ternary diagram of C_6–C_7 normal and isoalkane, cycloalkane, aromatic **(A)** and ternary diagram of nC_7, DMCP and MCH **(B)** in the TZ-I and ZB gas fields (modified from Hu et al., 2008).

the gases in the ZB gas field have experienced more actively oil cracking than those in TZ-I gas field.

Thermochemical Sulphate Reduction Degree

In most cases, TSR represents the only source that contributes high concentrations of H_2S to the deeply buried gas reservoirs (Orr, 1977; Worden and Smalley, 1996; Mougin et al., 2007; Hao et al., 2008). Worden et al. (1995) combined the gas source index (GSI), defined as $H_2S/(H_2S + \sum C_n)$, with total hydrocarbon gases to characterize the extent of TSR. Under the premise of sufficient sulfate concentration in reservoir, Hao et al. (2008) further proposed the three-stage TSR series corresponding to liquid-hydrocarbon-involved TSR, heavy-hydrocarbon-gas-dominated TSR and the methane-dominated TSR stage, respectively. In brief, the hydrocarbons are consumed and transformed to CO_2, H_2S, carbonate mineral if thermochemical sulphate reduction occurs in economic carbonate reservoir.

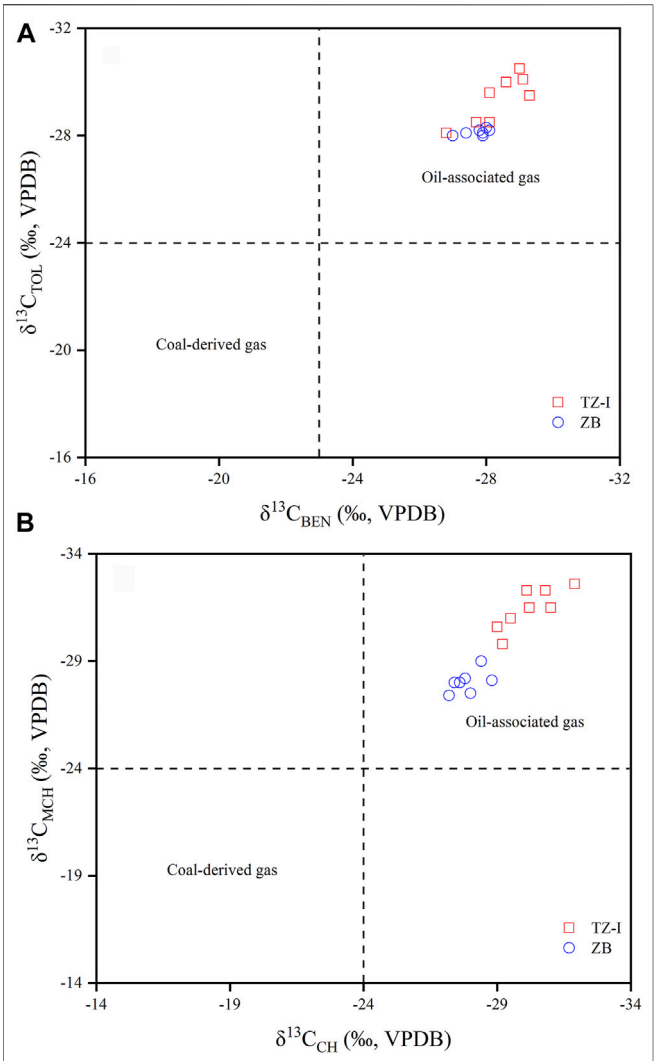

FIGURE 7 | $\delta^{13}C_{BEN}$ verse $\delta^{13}C_{TOL}$ **(A)**, $\delta^{13}C_{CH}$ verse $\delta^{13}C_{MCH}$ **(B)** cross plots of natural gases from TZ-I and ZB gas fields (modified from Hu et al., 2008).

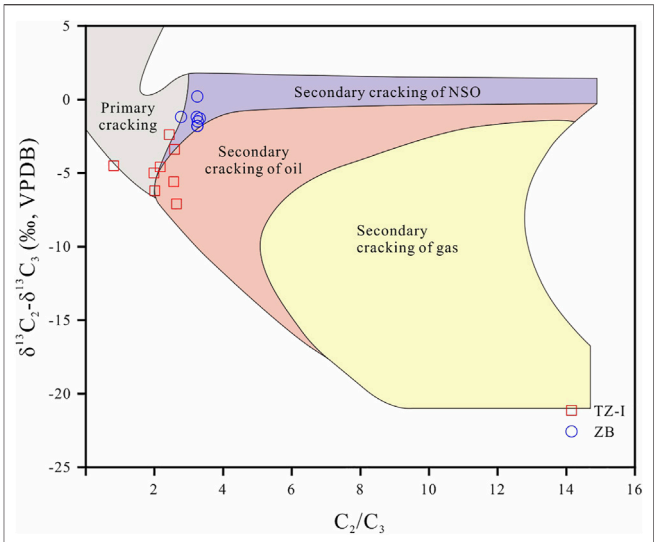

FIGURE 8 | The ($\delta^{13}C_2$-$\delta^{13}C_3$) and C_2/C_3 cross plot of natural gases from the TZ-I and ZB gas fields (Based on Prinzhofer et al., 2010).

Generally, the carbon isotope of CO_2 from TSR should be lighter due to the degradation of hydrocarbons.

Both the TZ-I and ZB gas fields have experienced TSR (Zhu et al., 2011; Cai et al., 2015), but the extent of the impact may have varied. The H_2S content of the gas in the TZ-I gas field was very low (<0.2%), and even in the gas with high maturity (TZ721 and TZ261 wells with dryness coefficients of >0.95), the content of H_2S was <0.05% (**Table 1**). Potentially, liquid-hydrocarbon-involved TSR did not significantly contribute to H_2S, which was found in the reservoirs (Hao et al., 2008). The concentration of total hydrocarbon gases in TZ-I gas field was still greater than 90%, implicitly demonstrating that the natural gases (C_1-C_4) rarely undergo heavy-hydrocarbon-gas-dominated or methane-dominated TSR (**Figure 9A**). Besides the disorder content relationship between CO_2 and GSI, a great discrepancy in the carbon isotope of CO_2 (from −11.9‰ to −2.8‰), suggesting that the CO_2 is controlled by other factors rather than a by-product of TSR (**Figure 9B**). Wu et al. (2014) suggested that the CO_2 with high $\delta^{13}C$ value in the natural gases were generated by mixing inorganic and organic CO_2. Some case studies (Krouse et al., 1988; Rooney et al., 1995; Worden and Smalley, 1996; Hao et al., 2008; Cai et al., 2015) and oxidation experiments (Pan et al., 2006) have suggested that the TSR affects the carbon isotope compositions of hydrocarbon gas to increase $\delta^{13}C$ of methane and ethane with increasing GSI. **Figures 9C,D** show that the carbon isotopes of methane and ethane in the TZ-I gas field were very light, and the carbon isotope ratios were rarely controlled by GSI, which was slightly affected by the TSR. The molecular compositions and isotopic characteristics all show that the gases in TZ-I gas field may be in the early liquid-hydrocarbon-involved TSR stage.

The gases of ZB gas field displayed high content H_2S (**Table 1**), and Zhu et al. (2011) suggested that TSR was most likely responsible for the occurrence of H_2S. The dryness coefficient of the gases in the ZB gas field was 0.97, with very low heavy hydrocarbon gas (**Table 1**). Besides, the decreasing content of total hydrocarbon gases was linearly associated with rising GSI (**Figure 9A**). These phenomena strongly showed that the methane, ethane and propane of the gases in the ZB gas field had been altered or consumed by TSR. Hence, there should be a certain amount of lighter CO_2 by hydrocarbon oxidation. The invariable content and very homogeneous carbon isotope of CO_2 in the ZB gas field indicated that the CO_2 was derived from a similar reaction or source, but its isotope was heavier beyond typical organic origin. Carbon dioxide in the ZB gas field may be mixed gas that is generated from TSR and carbonate decomposition under acidic conditions. Moreover, Worden and Smalley (1996) have indicated that elemental sulphur is an essential product of reactions between C_{2+} hydrocarbon gases and sulphate. The ^{12}C-rich C_{2+} gases were preferentially lost due to the weaker bond strengths of ^{12}C hydrocarbons (Krouse et al., 1988; Worden and Smalley, 1996). This phenomenon, in turn, triggers an increase in ^{13}C of ethane with increasing GSI. Elemental sulphur was only observed in sour gas reservoirs (Zhu et al., 2011), and the $^{13}C_2$ of associated gas is very

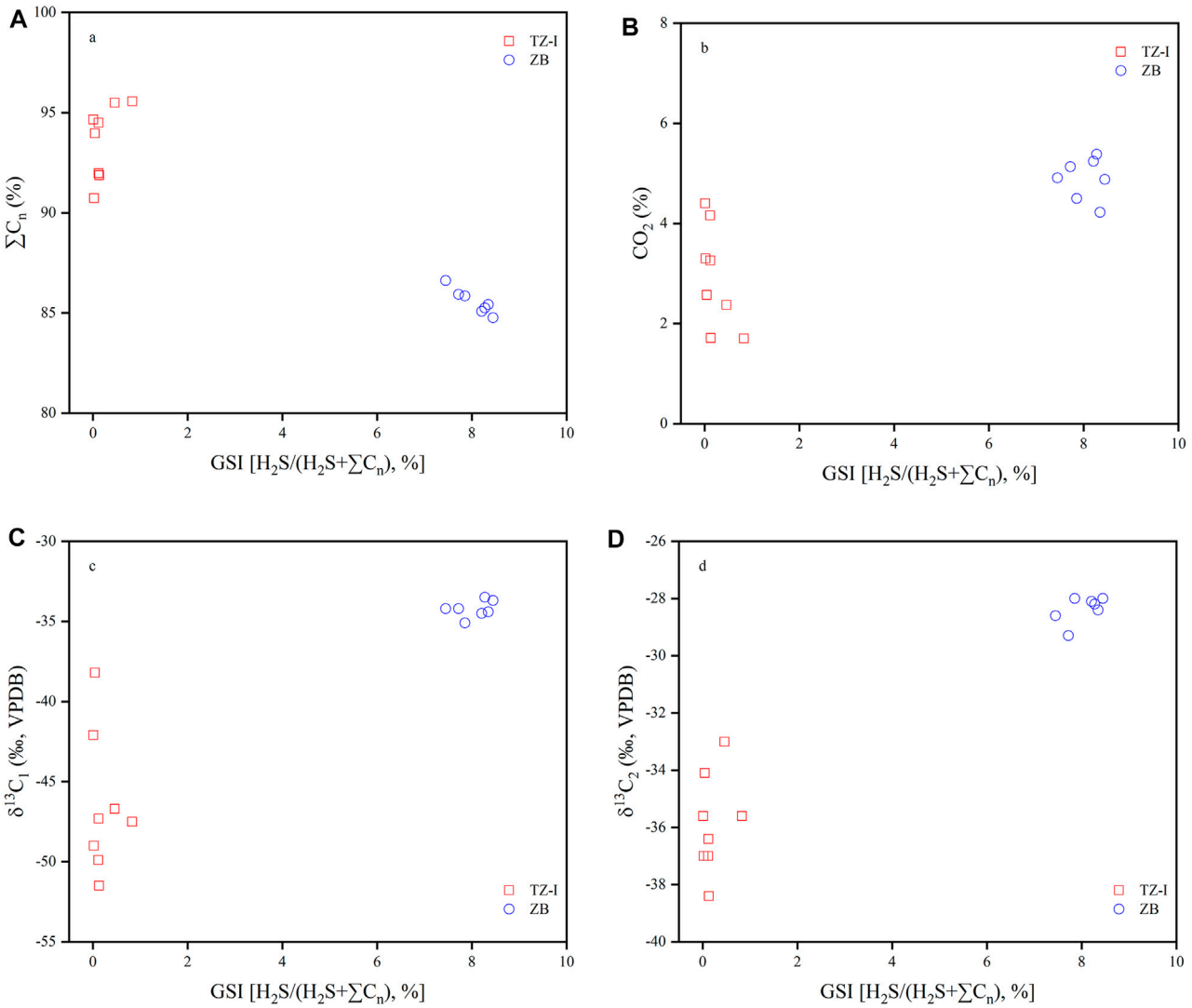

FIGURE 9 | Variation of $\sum C_n$ **(A)**, CO_2 **(B)**, $\delta^{13}C_1$ **(C)** and $\delta^{13}C_2$ **(D)** with gas souring index (GSI) for natural gases in the TZ-I and ZB gas fields, GSI = $H_2S/(H_2S+\sum C_n)$.

heavy. These findings further suggested that thermochemical sulphate reduction occurs in C_{2+}. As shown in **Figures 9C,D**, the $^{13}C_1$ has no significant variation with GSI, but the $^{13}C_2$ increasing enriched ^{13}C with the ascend of GSI. These characteristics were consistent with those of the heavy-hydrocarbon-gas-dominated TSR proposed by Hao et al. (2008) and indicated that methane-dominant TSR has barely happened yet. Therefore, the degree of TSR in the ZB gas field is in the stage of heavy-hydrocarbon-gas-dominated TSR and significantly differs from that in the TZ-I gas field. The latter was in the stage of the early liquid-hydrocarbon-involved TSR.

Effects of TSR on Carbon Isotope of Individual LHs

Whiticar and Snowdon (1999) have proposed that the carbon isotope ratios of the gasoline-range fraction (C_5-C_8) in Brazeau River condensate samples were strongly affected by TSR, the isotopic discrepancy among affected and unaffected specific compound even up to 10‰. In general, this induced the enrichment in ^{13}C for most compounds in TSR condensates relative to the samples less affected or unaffected by TSR (Rooney et al., 1995; Whiticar and Snowdon, 1999). Notably, the gases in the ZB and TZ-I gas fields were in different stages of TSR. Specifically, the gas in the TZ-I gas field was in the stage of the early liquid-hydrocarbon-involved TSR. Meanwhile, the gas in the ZB gas field was in the heavy-hydrocarbon-gas-dominated TSR. The carbon isotopes of individual LHs, associated with the gases in these two gas fields, indicated that TSR exerted a complex effect on the carbon isotopes of these individual LHs. Meanwhile, rather minor effect on the branch chain compounds 2-MP and 3-MP is identified. For instance, the $\delta^{13}C$ value of 2-MP in the TZ-I gas field was −28.6‰ on average, and that of the ZB gas field was

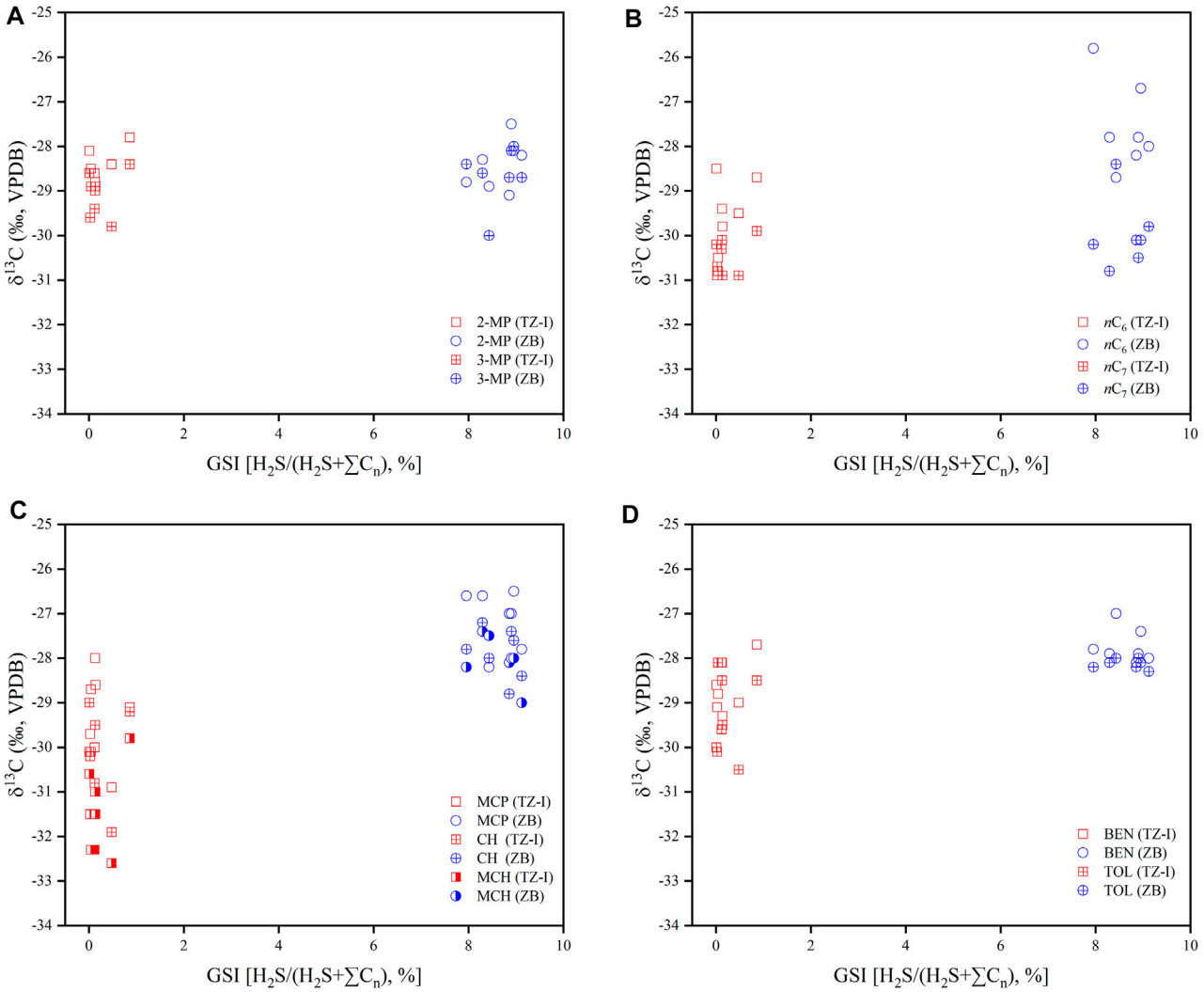

FIGURE 10 | The cross plot of $H_2S/(H_2S+\sum C_n)$ and ^{13}C for individual LHs [**(A)** 2-MP and 3-MP, **(B)** nC_5 and nC_6, **(C)** MCP, CH and MCH, **(D)** BEN and TOL] in the TZ-I and ZB gas fields.

−28.4‰. Thus, there was a slight difference (**Figure 10A**), which does not agree with the results from Whiticar and Snowdon (1999). They argued that TSR has a significant influence on the carbon isotopes of individual LHs. This disagreement was probably driven by the degree of TSR influence on the carbon isotopes of the individual LHs. During the liquid-hydrocarbon-involved and heavy-hydrocarbon-gas-dominated TSR stages, the TSR slightly affected the carbon isotopes of the individual LHs. For normal alkanes, there was also little effect by TSR (**Figure 10B**). However, for BEN and TOL carbon isotopes, it had been previously reported that maturity had little effect and was a good indicator for determining natural gas genetic types and gas sources (Li et al., 2003; Hu et al., 2008). The mean $\delta^{13}C$ values of BEN and TOL in the TZ-I gas field were −28.6‰ and −29.4‰, respectively, while those in the ZB gas field were −27.7‰ and −28.1‰, respectively. The comparative analysis of the two gas fields indicated that different degrees of TSR also slightly affected the carbon isotopes of BEN and TOL, about 1‰ (**Figure 10D**). Some relatively great differences in $\delta^{13}C$ for cyclocalkanes (2‰) were identified in these two gas fields, such as MCP, CH, and MCH (**Figure 10C**; **Table 3**). In the TZ-I gas field, the $\delta^{13}C$ values for MCP, CH, and MCH were −29.4‰, −30.2‰, −31.5‰ on average, respectively. As seen, they were more enriched ^{12}C than that in the ZB gas field during the hydrocarbon-gas-dominant TSR. Moreover, TSR was found to cause variations in the carbon isotopes of BEN and TOL, as well as cycloalkanes (**Figures 10C,D**). The carbon isotope of the above compound will be heavier with the TSR process. However, these variations were much lower than those of Whiticar and Snowdon (1999). The mechanism which caused the carbon isotope distribution discrepancy of normal, isoalkanes, cycloalkanes and aromatic compounds will be the focus on further research. Overall, the influence of TSR on the carbon isotopes of individual LHs should be considered, while using these carbon isotope indices to identify the

genetic type and source of marine natural gas, especially at the cut-off point ($\delta^{13}C$ = −24‰) of coal-derived gas and oil-associated gas.

CONCLUSION

The components and stable carbon isotope ratios of the C_1-C_4 and the individual LHs (C_6-C_7) in the gases from the TZ-I and ZB gas fields were used to examine the genetic type, oil cracking gas stage, TSR degree, and effects of TSR on carbon isotope of individual LHs. The main findings of this study are summarised below.

1) The $^{13}C_2$ of gases from the TZ-I gas field in Tarim Basin and ZB gas field in Sichuan Basin were always enriched ^{12}C (<-28.0‰), whereas the gases from the TZ-I gas field exhibited relatively lighter $\delta^{13}C_2$ values than those from the ZB gas field. The relative content of C_6-C_7 normal and iso-alkanes was found to be much greater than 30%. The gases were also located in the oil-associated area of the ternary diagram of C_7 LHs, which was similar to the distribution of C_6-C_7 LHs.The concentration of heptane was highest. The $\delta^{13}C_{BEN}$ and $\delta^{13}C_{TOL}$, $\delta^{13}C_{CH}$, and $\delta^{13}C_{MCH}$ values were < −26‰. These findings indicated that the gases in the TZ-I and ZB gas fields originated from the type II kerogen and were oil-associated gases.
2) The gases from the TZ-I and ZB gas fields were oil-cracking gases. It was demonstrated that the gas in the TZ-I gas field was in the early stage of oil cracking. The dryness coefficient of the gas in the ZB gas field was 0.97 and $\delta^{13}C_2$ value was higher than that in the TZ-I gas field. Meanwhile, the gas from the ZB gas field may have originated mainly from the secondary cracking stage of oil and wet gas.
3) The GSI value of gas from the TZ-I gas field was found to be very low, with quite a few heavy hydrocarbon gases and relatively lighter $\delta^{13}C_1$ and $\delta^{13}C_2$. This magnitude was somehow driven by TSR, and the gas may be in the early liquid carrier-involved TSR stage. The gas in the ZB gas field contained high contents of H_2S and CO_2 and lower C_{2+}. The carbon isotope of ethane becomes heavier as GSI increased. It was shown that the degree of TSR in the ZB gas field was in the heavy-hydrocarbon-gas-dominated TSR stage.
4) During the liquid-hydrocarbon-involved and heavy-hydrocarbon-gas-dominated TSR stages, the TSR slightly affected the carbon isotopes of individual LHs. Notably, TSR had a negligible effect on the branch chain compounds 2-MP and 3-MP and slightly affected on aromatic compound BEN and TOL. Meanwhile, greater effects (2‰) on carbon isotopes were identified for cycloalkanes such as MCP, CH, and MCH. The mechanism that caused these different phenomena will be the core for further research. To conclude, the carbon isotopes of individual LHs should be considered while using these indices to identify the genetic type and source of marine natural gas.

DATA AVAILABILITY STATEMENT

The original contributions presented in the study are included in the article/supplementary material, further inquiries can be directed to the corresponding author.

AUTHOR CONTRIBUTIONS

GH: manuscript writing. JG, LT, JS, and CF: manuscript discussion. XW: assistance in sample collection. ZL: assistance in sample analysis. All authors contributed to the article and approved the submitted version.

FUNDING

The first funding is a study about reservoir-forming rule and key exploration technology of large gas field which was funded by Petrochina Science and Technology Projects, and the Contract Number is 2021DJ0601. The second funding is a study on the carbon isotope composition and geochemical significance of light hydrocarbons in natural gas from the Sichuan Basin, and it was supported by National Natural Science Foundation of China (42172149).

ACKNOWLEDGMENTS

We thank Professor Jinxing Dai for long-standing help and associated Professor Wenlong Zhang for experiment help from the PetroChina Research Institute of Petroleum Exploration and Development.

REFERENCES

Behar, F., Kressmann, S., Rudkiewicz, J., and Vandenbroucke, M. (1992). Experimental Simulation in a Confined System and Kinetic Modelling of Kerogen and Oil Cracking. *Org. Geochem.* 19 (1-3), 173–189. doi:10.1016/0146-6380(92)90035-v

BeMent, W. O., Levey, R. A., and Mango, F. D. (1995). "The Temperature of Oil Generation as Defined with C7 Chemistry Maturity Parameter (2,4-Dmp/2,3-DMP Ratio)," in *Organic Geochemistry: Developments and Applications to Energy, Climate, Environment and Human History* (Donostian-San Sebastian: European Association of Organic Geochemists), 505–507.

Bernard, B. B., Brooks, J. M., and Sackett, W. M. (1978). Light Hydrocarbons in Recent Texas Continental Shelf and Slope Sediments. *J. Geophys. Res.* 83 (C8), 4053. doi:10.1029/jc083ic08p04053

Berner, U., and Faber, E. (1996). Empirical Carbon Isotope/maturity Relationships for Gases from Algal Kerogens and Terrigenous Organic Matter, Based on Dry, Open-System Pyrolysis. *Org. Geochem.* 24 (10-11), 947–955. doi:10.1016/s0146-6380(96)00090-3

Cai, C., Hu, G., Li, H., Jiang, L., He, W., Zhang, B., et al. (2015). Origins and Fates of H2S in the Cambrian and Ordovician in Tazhong Area: Evidence from Sulfur Isotopes, Fluid Inclusions and Production Data. *Mar. and Petroleum Geol.* 67, 408–418. doi:10.1016/j.marpetgeo.2015.05.007

Cai, C., Hu, W., and Worden, R. H. (2001). Thermochemical Sulphate Reduction in Cambro-Ordovician Carbonates in Central Tarim. *Mar. and Petroleum Geol.* 18 (6), 729–741. doi:10.1016/s0264-8172(01)00028-9

Cai, C., Zhang, C., Cai, L., Wu, G., Jiang, L., Xu, Z., et al. (2009). Origins of Palaeozoic Oils in the Tarim Basin: Evidence from Sulfur Isotopes and Biomarkers. *Chem. Geol.* 268 (3-4), 197–210. doi:10.1016/j.chemgeo.2009.08.012

Dai, J. (1993). Identification of Coal Formed Gas and Oil Type Gas by Light Hydrocarbons. *Petroleum Explor. Dev.* 20 (5), 26–32. (in Chinese with English abstract).

Dai, J., Li, J., Luo, X., Zhang, W., Hu, G., Ma, C., et al. (2005). Stable Carbon Isotope Compositions and Source Rock Geochemistry of the Giant Gas Accumulations in the Ordos Basin, China. *Org. Geochem.* 36 (12), 1617–1635. doi:10.1016/j.orggeochem.2005.08.017

Dai, J., Ni, Y., Huang, S., Gong, D., Liu, D., Feng, Z., et al. (2016). Secondary Origin of Negative Carbon Isotopic Series in Natural Gas. *J. of Nat. Gas Geoscience* 1 (1), 1–7. doi:10.1016/j.jnggs.2016.02.002

Dai, J., Song, Y., Chen, K., Hong, F., and &Fan, G. (1992). Characteristics of Carbon Isotopes of Organic Alkane Gases in Petroliferous Basins of China. *J. of Petroleum Sci. and Eng.* 7 (3-4), 329–338.

Dai, J., Xia, X., Li, Z., Coleman, D. D., Dias, R. F., Gao, L., et al. (2012). Inter-laboratory Calibration of Natural Gas Round Robins for δ2H and δ13C Using Off-Line and On-Line Techniques. *Chem. Geol.* 310-311, 49–55. doi:10.1016/j.chemgeo.2012.03.008

George, S. C., Boreham, C. J., Minifie, S. A., and Teerman, S. C. (2002). The Effect of Minor to Moderate Biodegradation on C 5 to C 9 Hydrocarbons in Crude Oils. *Org. Geochem.* 33 (12), 1293–1317. doi:10.1016/s0146-6380(02)00117-1

Guan, B., Zhang, C., Li, S., Han, J., Zhao, L., and Xiong, C. (2020). Three-stage Reservoir Unit Description and Benefit Development of Fracture-Controlled Cave Carbonate Reservoirs in Tazhong Uplift, Tarim Basin. *Nat. Gas. Geosci.* 31 (12), 1766–1778. (in Chinese with English abstract). doi:10.11764/j.issn.1672-1926.2020.04.009

Hao, F., Guo, T., Zhu, Y., Cai, X., Zou, H., and Li, P. (2008). Evidence for Multiple Stages of Oil Cracking and Thermochemical Sulfate Reduction in the Puguang Gas Field, Sichuan Basin, China. *Bulletin* 92 (5), 611–637. doi:10.1306/01210807090

Hill, R. J., Tang, Y., and Kaplan, I. R. (2003). Insights into Oil Cracking Based on Laboratory Experiments. *Org. Geochem.* 34 (12), 1651–1672. doi:10.1016/s0146-6380(03)00173-6

Hu, G., Li, J., and Li, J. (2008). Preliminary Study on the Origin Identification of Natural Gas by Parameters of Light Hydrocarbon. *Sci. China Ser. D Earth Sci.* 51 (S1), 131–139. doi:10.1007/s11430-008-5017-x

Hu, G., Li, J., Xie, Z., and Yu, C. (2018). *Geochemistry of Light Hydrocarbons Associated with Natural Gas*. Beijing: Petroleum Industry Press. (in Chinese with English abstract).

Hu, G., and Zhang, S. (2011). Characterization of Low Molecular Weight Hydrocarbons in Jingbian Gas Field and its Application to Gas Sources Identification. *Energy Explor. Exploitation* 29 (6), 777–795. doi:10.1260/0144-5987.29.6.777

Hu, T., Ge, B., and Zhang, Y. (1990). The Development and Application of Fingerprint Parameters for Hydrocarbons Absorbed by Source Rocks and Light Hydrocarbon in Natural Gas. *Petroleum Explor. Dev.* 12 (4), 375–379. (in Chinese with English abstract).

Jenden, P., Newell, K., Kaplan, I., and Watney, W. (1988). Composition and Stable-Isotope Geochemistry of Natural Gases from Kansas, Midcontinent, U.S.A. *Chem. Geol.* 71 (1-3), 117–147. doi:10.1016/0009-2541(88)90110-6

Jiang, Z., Luo, X., Li, Z., Zhang, Y., and Pang, X. (2000). Carbon Isotope Composition of Benzene and Toluene as a New Index for Correlation of Gases with Their Source Rocks. *Geochemica* 29 (4), 410–415. (in Chinese with English abstract). doi:10.19700/j.0379-1726.2000.04.015

Krouse, H. R., Viau, C. A., Eliuk, L. S., Ueda, A., and Halas, S. (1988). Chemical and Isotopic Evidence of Thermochemical Sulphate Reduction by Light Hydrocarbon Gases in Deep Carbonate Reservoirs. *Nature* 333 (6172), 415–419. doi:10.1038/333415a0

Li, J., Luo, X., Li, Z. S., Jiang, Z., Hu, G., and Xie, Z. (2003). Carbon Isotope Value of Toluene as a New Index for Correlation of Gases with Their Source Rocks. *Nat. Gas. Geosci.* 14 (3), 177–180. (in Chinese with English abstract). doi:10.11764/j.issn.1672-1926.2003.03.117

Liang, D., Zhang, S., Zhao, M., and Wang, F. (2002). Hydrocarbon Sources and Stages of Reservoir Formation in Kuqa Depression, Tarim Basin. *Chin. Sci. Bull.* 47 (S1), 62–70. doi:10.1007/bf02902820

Liao, F., Yu, C., Wu, W., and Liu, D. (2014). Stable Carbon and Hydrocarbon Isotopes of Natural Gas from the Zhongba Gas Field in the Sichuan Basin and Implication for Gas-Source Correlation. *Nat. Gas. Geosci.* 25 (1), 79–86. (in Chinese with English abstract). doi:10.11764/j.issn.1672-1926.2014.01.0079

Liu, Q. Y., Worden, R. H., Jin, Z. J., Liu, W., Li, J., Gao, B., et al. (2013). TSR Versus Non-TSR Processes and Their Impact on Gas Geochemistry and Carbon Stable Isotopes in Carboniferous, Permian and Lower Triassic Marine Carbonate Gas Reservoirs in the Eastern Sichuan Basin, China. *Geochim. Cosmochim. Acta* 100 (1), 96–115.

Lorant, F., Prinzhofer, A., Behar, F., and Huc, A. (1998). Carbon Isotopic and Molecular Constraints on the Formation and the Expulsion of Thermogenic Hydrocarbon Gases. *Chem. Geol.* 147 (3-4), 249–264. doi:10.1016/s0009-2541(98)00017-5

Mango, F. (1997). The Light Hydrocarbons in Petroleum: a Critical Review. *Org. Geochem.* 26 (7-8), 417–440. doi:10.1016/s0146-6380(97)00031-4

Mougin, P., Lamoureux-Var, V., Bariteau, A., and Huc, A. (2007). Thermodynamic of Thermochemical Sulphate Reduction. *J. of Petroleum Sci. and Eng.* 58 (3-4), 413–427. doi:10.1016/j.petrol.2007.01.005

Orr, W. L. (1997). *Geologic and Geochemical Controls on the Distribution of Hydrogen Sulfide in Natural Gas: Advances in Organic Geochemistry: Madrid, Enadisma*, 571–597.

Pan, C., Yu, L., Lui, J., and Fu, J. (2006). Chemical and Carbon Isotopic Fractionations of Gaseous Hydrocarbons during Abiogenic Oxidation. *Earth and Planet. Sci. Lett.* 246 (1-2), 70–89. doi:10.1016/j.epsl.2006.04.013

Prinzhofer, A., and Rocha, M. (2000). Geochemical Characterization of Natural Gas: A Physical Multivariable Approach and its Applications in Maturity and Migration Estimates. *AAPG Bul.* 84, 1152–1172. doi:10.1306/a9673c66-1738-11d7-8645000102c1865d

Prinzhofer, A., Dos Santos Neto, E. V., and Battani, A. (2010). Coupled Use of Carbon Isotopes and Noble Gas Isotopes in the Potiguar Basin (Brazil): Fluids Migration and Mantle Influence. *Mar. and Petroleum Geol.* 27 (6), 1273–1284. doi:10.1016/j.marpetgeo.2010.03.004

Prinzhofer, A., and Huc, A. (1995). Genetic and Post-genetic Molecular and Isotopic Fractionations in Natural Gases. *Chem. Geol.* 126 (3-4), 281–290. doi:10.1016/0009-2541(95)00123-9

Rooney, M., Claypool, G., and Moses Chung, H. (1995). Modeling Thermogenic Gas Generation Using Carbon Isotope Ratios of Natural Gas Hydrocarbons. *Chem. Geol.* 126 (3-4), 219–232. doi:10.1016/0009-2541(95)00119-0

Stahl, W. J., and Carey, B. D. (1975). Source-rock Identification by Isotope Analyses of Natural Gases from Fields in the Val Verde and Delaware Basins, West Texas. *Chem. Geol.* 16 (4), 257–267. doi:10.1016/0009-2541(75)90065-0

Tassi, F., Bonini, M., Montegrossi, G., Capecchiacci, F., Capaccioni, B., and Vaselli, O. (2012). Origin of Light Hydrocarbons in Gases from Mud Volcanoes and CH4-Rich Emissions. *Chem. Geol.* 294-295, 113–126. doi:10.1016/j.chemgeo.2011.12.004

Tian, H., Xiao, X. M., Li, X. Q., Xiao, Z. Y., Shen, J. Q., and Liu, D. H. (2007). Comparison of Gas Generation and Carbon Isotope Fractionation of Methane From Marine Kerogen- and Crude Oil-Cracking Gases. *Geochimica* 36 (1), 71–77. (in Chinese with English abstract)

Thompson, K. F. M. (1983). Classification and Thermal History of Petroleum Based on Light Hydrocarbons. *Geochimica Cosmochimica Acta* 47 (2), 303–316. doi:10.1016/0016-7037(83)90143-6

Tilley, B., and Muehlenbachs, K. (2013). Isotope Reversals and Universal Stages and Trends of Gas Maturation in Sealed, Self-Contained Petroleum Systems. *Chem. Geol.* 339, 194–204. doi:10.1016/j.chemgeo.2012.08.002

Vieth, A., and Wilkes, H. (2006). Deciphering Biodegradation Effects on Light Hydrocarbons in Crude Oils Using Their Stable Carbon Isotopic Composition: A Case Study from the Gullfaks Oil Field, Offshore Norway. *Geochimica Cosmochimica Acta* 70 (3), 651–665. doi:10.1016/j.gca.2005.08.022

Wang, Z., Su, J., Zhu, G., Han, J., and Wang, Y. (2013). Characteristics and Accumulation Mechanism of Quasi-Layered Ordovician Carbonate Reservoirs in the Tazhong Area, Tarim Basin. *Energy Explor. Exploitation* 31 (4), 545–567. doi:10.1260/0144-5987.31.4.545

Welte, D. H., Kratochvil, H., Rullkötter, J., Ladwein, H., and Schaefer, R. G. (1982). Organic Geochemistry of Crude Oils from the Vienna Basin and an Assessment of Their Origin. *Chem. Geol.* 35, 33–68. doi:10.1016/0009-2541(82)90018-3

Whiticar, M. J., and Snowdon, L. R. (1999). Geochemical Characterization of Selected Western Canada Oils by C5–C8 Compound Specific Isotope Correlation (CSIC). *Org. Geochem.* 30 (9), 1127–1161. doi:10.1016/s0146-6380(99)00093-5

Worden, R., and Smalley, P. (1996). H_2S-producing Reactions in Deep Carbonate Gas Reservoirs: Khuff Formation, Abu Dhabi. *Chem. Geol.* 133 (1-4), 157–171. doi:10.1016/s0009-2541(96)00074-5

Worden, R. H., Smalley, P. C., and Oxtoby, N. H. (1995). Gas Souring by Thermochemical Sulfate Reduction at 140°C. *AAPG Bull.* 79, 854–863.

Wu, X., Tao, X., and Hu, G. (2014). Geochemical Characteristics and Genetic Types of Natural Gas from Tazhong Area in the Tarim Basin, NW China. *Energy Explor. Exploitation* 32 (1), 159–174. doi:10.1260/0144-5987.32.1.159

Xiao, Z., Xie, Z., Li, Z., and Ma, C. (2008). Isotopic Characteristics of Natural Gas of Xujiahe Formayion in Southern and Middle of Sichuan Basin. *Geochimica* 37 (3), 245–250. (in Chinese with English abstract). doi:10.19700/j.0379-1726.2008.03.007

Xiao, Q., Sun, Y., Zhang, Y., and Chai, P. (2012). Stable Carbon Isotope Fraction of Individual Light Hydrocarbons in the C6-C8 Range in Crude Oil as Induced by Natural Evaporation: Experimental Results and Geological Implications. *Org. Geochem.* 50, 44–56

Yang, H., Han, J., Chen, L., Wu, C., and Ji, Y. (2007). Characteristics and Patterns of Complex Hydrocarbon Accumulation in the Lower Paleozoic Carbonate Rocks of the Tazhong Paleouplift. *Oil and Gas Geology* 28 (6), 784–790. (in Chinese with English abstract)

Zhao, W., Zhu, G., Zhang, S., Zhao, X., Sun, Y., Wang, H., et al. (2009). Relationship between the Later Strong Gas-Charging and the Improvement of the Reservoir Capacity in Deep Ordovician Carbonate Reservoir in Tazhong Area, Tarim Basin. *Chin. Sci. Bull.* 54 (17), 3076–3089. doi:10.1007/s11434-009-0457-z

Zhou, X. (2013). Accumulation Mechanism of Complicated Deep Carbonate Reservoir in the Tazhong Area, Tarim Basin. *Energy Explor. Exploitation* 31 (3), 429–457. doi:10.1260/0144-5987.31.3.429

Zhu, G., Zhang, S., Huang, H., Liang, Y., Meng, S., and Li, Y. (2011). Gas Genetic Type and Origin of Hydrogen Sulfide in the Zhongba Gas Field of the Western Sichuan Basin, China. *Appl. Geochem.* 26 (7), 1261–1273. doi:10.1016/j.apgeochem.2011.04.016

Conflict of Interest: Authors GH, JG, LT, JS, ZL and CF were employed by the company PetroChina. Author XW was employed by the company Sinopec.